

Critical phenomena and quantum statistics in the four-wave interaction

G. Yu. Kryuchkyan and K. V. Kheruntsyan

Institute of Physical Studies, Armenian National Academy of Sciences, 378410 Ashtarak-2, Republic of Armenia

(Submitted 31 August 1995; resubmitted 10 April 1996)

Zh. Éksp. Teor. Fiz. **110**, 1589–1607 (November 1996)

We develop a theory of intracavity four-wave interaction. As a result of such interaction, two photons of the pump fields produce a pair of photons of the cavity's signal mode with the same frequency. In addition to taking into account the parametric process of photon transformation and dissipation processes, we allow for the effects of phase self-modulation of the signal mode and its cross modulation due to the pump fields. We find an exact steady-state solution of the Fokker–Planck equation for the distribution function of the quasiprobability of the amplitude in the generalized P -representation of the density matrix. This solution is then used to calculate the moments of the signal-mode operators, the distribution function for the number of photons, and the Wigner function. The results are applicable to all oscillating modes, including the threshold and above-threshold regions and the bistable mode. We study critical phenomena and the quantum statistical effects of photon correlation, the squeezing of fluctuations of the quadrature component, and sub-Poisson statistics. We find, in particular, that the pair correlation of photons increases significantly in the threshold region with the bistable oscillating mode present. We also show that squeezing in the threshold region is manifested only in the absence of bistability. Finally, we analyze the threshold characteristics of the nonlinear system and the characteristic features of the transition to nonthreshold behavior at high levels of quantum noise and large nonlinearities. © 1996 American Institute of Physics. [S1063-7761(96)00411-8]

1. INTRODUCTION

An important problem that emerges while investigating nonlinear processes in quantum optics is the study of properties of the light fields generated in the vicinity of various critical points, such as the lasing threshold and points of metastability and instability, where quantum fluctuations play an important role. The problem is common in the QED theory of lasing and in studying optical bistability phenomena with analogs in phase transition theory. Recently new problems have emerged in this area of research, problems related to the description of the properties of nonclassical states of light—specifically squeezed states—in critical (above-threshold) regions of generation of such states.

Nonlinear systems in quantum optics are usually studied by applying the method of stochastic Langevin equations of motion for the complex-valued amplitudes of the generated fields combined with a linearization procedure near semiclassical solutions. Such an approach was used in studying the main nonlinear optics process, including parametric frequency division of the light in the cavity,^{1–7} four-wave mixing,^{7–10} second-harmonic generation,^{1,6,11} etc.^{12,13} It leads to results for the intensities and phases of the interacting modes of the light field in the semiclassical approximation and also makes it possible to study quantum fluctuation effects in the lowest linear approximation. Actually, the very notion of a critical point or a lasing threshold emerges in a natural manner in such an approach when one analyzes the stability of the semiclassical steady-state equations for the amplitudes.

Clearly, linearized theories are limited in scope and, in particular, do not describe the critical region, where the

quantum fluctuation levels are usually very high. To allow for quantum fluctuations in a meaningful manner with the aim of building an exact quantum theory of nonlinear optical processes, we can use the solutions of the Fokker–Planck equation for the quasiprobability distribution function. The pioneering work in this field was done in Refs. 1(b) and 14–17, where the generalized P -representation of the density matrix was used to study two-photon absorption, nonlinear dispersion or phase self-modulation in the cavity, subharmonic and second-harmonic generation, and nondegenerate parametric frequency division of the light in the cavity. Finding the quasiprobability distributions is extremely difficult, however, and solutions that are exact in quantum fluctuations have been established only for relatively simple systems.

In this paper we give a new example of a nonlinear optics system for which an exact analysis of the problem is possible and results can be obtained within the scope of the nonlinear quantum-fluctuation theory. We discuss parametric four-wave interaction in a $\chi^{(3)}$ -nonlinear medium in a cavity, induced by two laser pump fields with frequencies ω_1 and ω_2 , for the case in which one mode with a frequency close to $\omega_0 = (\omega_1 + \omega_2)/2$ is excited in the cavity ($\omega_1 + \omega_2 \rightarrow \omega_0 + \omega_0$). If we employ the approximation of inexhaustible pump sources, then in addition to the parametric excitation of the signal mode ω_0 , we take into account phase self-modulation of the signal mode and its cross modulation due to the pump fields.

This system has been studied by the present authors in approximations that are semiclassical and linear in quantum fluctuations.^{18,19} It was found that this situation leads to above-threshold lasing even when the energy exchange be-

tween the modes is negligible, with the sources of pump fields inexhaustible. The physical reason for such a lasing mode is the existence and stabilizing effect of phase self-modulation of the signal mode. We also note that signal-mode generation in a similar configuration with four-wave interaction was observed in the experiments of Grandclement *et al.*²⁰

The aim of the present work is to develop an exact quantum theory for the specified nonlinear optics system in a stationary regime that allows for energy dissipation, and to examine critical phenomena. We also study the quantum statistical effects of quadrature-component fluctuation squeezing, photon correlation, and the distribution of the number of photons for the generated signal mode over the entire lasing range, including the threshold and above-threshold regions. We attempt to establish how bistability in the quantum statistical characteristics of the signal mode is induced; how nonclassical effects show up in the critical region, where quantum noise plays a large role; and finally, what features are inherent in the four-wave interaction in highly nonlinear media. From a fundamental viewpoint, interest in the nonlinear optics system discussed here can also be explained by the fact that this system clearly exemplifies the transition from classical behavior to quantum behavior.

2. THE FOUR-WAVE INTERACTION AND THE FOKKER-PLANCK EQUATION

The system we are considering here consists of a cubic-nonlinear $\chi^{(3)}$ -medium in a single-mode ring cavity with natural frequency ω_c . Two laser pump fields of frequency ω_1 and ω_2 propagate in the same direction in the cavity and act on the medium. As a result of parametric four-wave mixing, the pump fields excite a signal mode in the cavity ($\omega_1 + \omega_2 \rightarrow \omega_0 + \omega_0$) if the frequency $\omega_0 = (\omega_1 + \omega_2)/2$, which is determined by the phase-locking condition, is close to the resonant frequency ω_c . Here the cavity is assumed transparent at the pump frequencies, and the pump fields are thought of as being inexhaustible and obeying classical field theory. The signal mode of the cavity is described quantum mechanically and, in addition to taking into account the four-wave mixing process, we allow for phase self-modulation and phase cross-modulation due to the pump fields. These effects emerge in a natural way in the interaction of waves in a $\chi^{(3)}$ -medium, but are often ignored in elementary descriptions of the four-wave interaction. However (see, e.g., Refs. 21 and 22), allowing for them can lead to significant changes in the four-wave interaction in comparison to a "pure" parametric process.

The system Hamiltonian in the resonance approximation with mode damping in the cavity can be written in the following form:¹⁹

$$H = \hbar \omega_c a^\dagger a + H_{\text{eff}} + a^\dagger \Gamma + a \Gamma^\dagger, \quad (1)$$

$$H_{\text{eff}} = \frac{\hbar \chi}{2} (a^2 E_1^* E_2^* e^{i(\omega_1 + \omega_2)t} + a^{\dagger 2} E_1 E_2 e^{-i(\omega_1 + \omega_2)t}) + \frac{\hbar \chi}{4} a^{\dagger 2} a^2 + \hbar \chi (|E_1|^2 + |E_2|^2) a^\dagger a.$$

Here the first term is the free part of the Hamiltonian, where a^\dagger and a are the signal-mode creation and annihilation operators. The terms of the effective Hamiltonian H_{eff} describe, respectively, parametric four-wave mixing and phase self-modulation of the signal mode and its cross modulation due to the pump fields. In the expression for H_{eff} the coupling constant χ is proportional to the third-order susceptibility $\chi^{(3)}$, and E_1 and E_2 are the complex-valued amplitudes of the pump fields. The last two terms in (1) describe mode damping in the cavity in terms of the thermostat operators Γ and Γ^\dagger , which determine the damping factor γ .

Following the standard procedure (see, e.g., Refs. 13 and 23) of eliminating the thermostat variables combined with a transformation to operators that slowly vary in time,

$$a(t) \rightarrow a e^{-i\omega_0 t}, \quad a^\dagger(t) \rightarrow a^\dagger e^{i\omega_0 t}, \quad (2)$$

we use Eq. (1) to obtain the following equation for the density matrix ρ in the interaction picture:

$$\begin{aligned} \frac{\partial \rho}{\partial t} = & i\Delta [a^\dagger a, \rho] - \frac{i\chi}{2} (E_1^* E_2^* [a^2, \rho] + E_1 E_2 [a^{\dagger 2}, \rho]) \\ & - \frac{i\chi}{4} [a^{\dagger 2} a^2, \rho] - i\chi (|E_1|^2 + |E_2|^2) [a^\dagger a, \rho] \\ & + \gamma (2a\rho a^\dagger - \rho a^\dagger a - a^\dagger a\rho), \end{aligned} \quad (3)$$

where $\Delta = \omega_0 - \omega_c$ is the detuning of the cavity, and we have ignored the contribution of thermal fluctuations on the assumptions that the temperature of the thermostat is low ($kT \ll \hbar\omega$). Equation (3) is used to obtain the Fokker-Planck equation for the quasiprobability distribution function $P(\alpha, \beta)$ in the generalized complex-valued P -representation^{14,24} of the density matrix:

$$\rho = \int d\alpha \int d\beta \frac{|\alpha\rangle \langle \beta^*|}{\langle \beta^* | \alpha \rangle} P(\alpha, \beta), \quad (4)$$

where $|\alpha\rangle$ and $|\beta^*\rangle$ are coherent states, with $a|\alpha\rangle = \alpha|\alpha\rangle$ and $\langle \beta^* | a^\dagger = \beta \langle \beta^* |$. In contrast to the diagonal Glauber-Sudarshan P -representation, in the complex-valued P -representation the quantities α and β are independent complex-valued c -number variables ($\beta \neq \alpha^*$) corresponding to the operators a and a^\dagger , and integration with respect to these variables must be carried out along separate contours. The Fokker-Planck equation for the distribution $P(\alpha, \beta)$ can be obtained from (3) in the standard manner,^{13,24} and has the form

$$\frac{\partial}{\partial t} P(\alpha) = \left[\frac{\partial}{\partial \alpha_\mu} A_\mu + \frac{1}{2} \frac{\partial^2}{\partial \alpha_\mu \partial \alpha_\nu} D_{\mu\nu} \right] P(\alpha), \quad (5)$$

where we have used the vector notation $\alpha = (\alpha_1, \alpha_2) = (\alpha, \beta)$, and $\mu, \nu = 1, 2$. The coefficients A_1 and A_2 in (5) are

$$\begin{aligned} A_1 = & \gamma\alpha - i[\Delta - \chi(|E_1|^2 + |E_2|^2)]\alpha \\ & + \frac{i\chi}{2}\beta\alpha^2 + i\chi E_1 E_2 \beta, \end{aligned} \quad (6a)$$

$$A_2 = \gamma\beta + i[\Delta - \chi(|E_1|^2 + |E_2|^2)]\beta$$

$$-\frac{i\chi}{2}\alpha\beta^2 - i\chi E_1^* E_2^* \alpha, \quad (6b)$$

and the $D_{\mu\nu}$ are the elements of the following diffusion matrix:

$$D = \begin{pmatrix} -i\chi(E_1 E_2 + \frac{1}{2}\alpha^2) & \vdots & 0 \\ \dots\dots\dots & \cdot & \dots\dots\dots \\ 0 & \vdots & i\chi(E_1^* E_2^* + \frac{1}{2}\beta^2) \end{pmatrix}. \quad (7)$$

3. STEADY-STATE QUASIPROBABILITY DISTRIBUTION AND THE MOMENTS OF THE SIGNAL-MODE OPERATORS

Finding exact quantum statistical results that describe the behavior of the system in the critical regions and in the presence of quantum noise of arbitrary intensity requires solving the Fokker–Planck equation (5) in a time-independent setting exactly and calculating the normal-ordered moments of the signal-mode operators

$$\langle a^{+m} a^n \rangle = \int_C \int_{C'} d\alpha d\beta \alpha^m \beta^n P(\alpha, \beta), \quad (8)$$

$$\langle a^{+m} a^n \rangle = \frac{\sum_{k=0}^{\infty} \frac{2^k}{k!} \int_C d\alpha \alpha^{k+n} (\alpha^2 + 2E_1 E_2)^\lambda \int_{C'} d\beta \beta^{k+m} (\beta^2 + 2E_1^* E_2^*)^{\lambda*}}{\sum_{k=0}^{\infty} \frac{2^k}{k!} \int_C d\alpha \alpha^k (\alpha^2 + 2E_1 E_2)^\lambda \int_{C'} d\beta \beta^k (\beta^2 + 2E_1^* E_2^*)^{\lambda*}}. \quad (11)$$

Clearly, the contour integrals in (11) are similar to the following integral representation of the (complete) beta function $B(z_1, z_2)$ of complex variables:²⁵

$$\int_C t^a (t^2 - 1)^b dt = \begin{cases} 0 & \text{for } a \text{ odd,} \\ 2i \sin(\pi b) B\left(b + 1, \frac{a+1}{2}\right) & \text{for } a \text{ even,} \end{cases} \quad (12)$$

where the contour C is a figure eight encompassing the points $t = \pm 1$. This leads to the following result for arbitrary moments (8) in the stationary regime:

$$\langle a^{+m} a^n \rangle = \frac{M_{mn}}{M_{00}}, \quad (13)$$

$$M_{mn} = (-2E_1 E_2)^{n/2} (-2E_1^* E_2^*)^{m/2} \times \sum_{k=0}^{\infty} \frac{|4E_1 E_2|^k}{k!} [1 + (-1)^{k+n}] [1 + (-1)^{k+m}] \times B\left(\lambda + 1, \frac{k+n+1}{2}\right) B\left(\lambda^* + 1, \frac{k+m+1}{2}\right). \quad (14)$$

Below we discuss expressions (13) and (14) for the special cases describing the intensity and second-order signal-mode moments.

where C and C' are the integration contours.

To find the steady-state solution $P_s(\alpha, \beta)$ of Eq. (5), we use the method of potential equations.^{13,24} We can easily verify that this solution of the Fokker–Planck equation with the coefficients (6) and the diffusion matrix (7) does exist, since the appropriate potential conditions are met:

$$P_s(\alpha, \beta) = N (\alpha^2 + 2E_1 E_2)^\lambda (\beta^2 + 2E_1^* E_2^*)^{\lambda*} e^{2\alpha\beta}, \quad (9)$$

where

$$\lambda = -1 - \frac{2\Delta}{\chi} + 2(|E_1|^2 + |E_2|^2) - \frac{2i\gamma}{\chi}, \quad (10)$$

and N is a normalization constant.

Plugging this solution into (8) and expanding the exponential $\exp(2\alpha\beta)$ in a power series separates the variables in the integrals. Combining this with the normalization condition yields

4. STEADY-STATE INTENSITY

In this section we study the average intensity of the generated signal mode at the cavity output in the steady state:

$$I^{\text{out}} = \langle a_{\text{out}}^+ a_{\text{out}} \rangle = 2\gamma \langle a^+ a \rangle$$

(here a_{out} is the field operator at the cavity output²⁶). Expressing the beta function in (13) and (14) in terms of gamma functions, $B(x, y) = \Gamma(x)\Gamma(y)/\Gamma(x+y)$, using the well-known properties of the latter, and performing some simple transformations, we obtain

$$I^{\text{out}} = \frac{2\gamma M'_{11}}{M'_{00}}, \quad (15)$$

$$M'_{00} = \frac{1}{1 + (J_1 + J_2 - d - \delta)^2} + \sum_{k=1}^{\infty} \frac{(2k-1)!!}{(2k)!!} (J_1 J_2)^k \left(\prod_{j=1}^{k+1} P_j \right)^{-1}, \quad (16)$$

$$M'_{11} = \frac{J_1 J_2}{2} \sum_{k=0}^{\infty} \frac{(2k+1)!!}{(2k)!!} (J_1 J_2)^k \left(\prod_{j=1}^{k+2} P_j \right)^{-1}, \quad (17)$$

where

$$P_j = 1 + (J_1 + J_2 - d - 3\delta + 2j\delta)^2. \quad (18)$$

Here the moments M'_{mn} differ from the moments (14) by a constant factor,

$$M'_{mn} = \frac{16\pi\delta^2|\lambda|^2\Gamma(\lambda)\Gamma(\lambda^*)}{\Gamma(\lambda+1/2)\Gamma(\lambda^*+1/2)} M'_{mn}, \quad (19)$$

and we have introduced the dimensionless parameters

$$J_{1,2} = \frac{\chi}{\gamma} I_{1,2}, \quad d = \frac{\Delta}{\gamma}, \quad \delta = \frac{\chi}{4\gamma}, \quad (20)$$

where $I_{1,2} = |E_{1,2}|^2$ are the pump field intensities.

Now let us turn to the results of numerical analysis of the intensities via (15)–(17) in graphical form for equal pump intensities, $I_1 = I_2 \equiv I$ ($J_1 = J_2 \equiv J$). Figure 1 (curves 1 and 2) depicts the dependence of $J^{\text{out}} = \chi I^{\text{out}}/4\gamma^2$ on J for various values of d and δ . A increase (decrease) in d leads to an increase (decrease) in I^{out} , and also to broadening (narrowing) of the range of signal generation at some significant intensity.

Having in mind subsequent discussions, we also give the results obtained in semiclassical theory and in an approximation that is linear in quantum fluctuations.¹⁹

The semiclassical equations of motion and an analysis of stability of their steady-state solutions under small fluctuations suggest two stable solutions for the amplitude α_0 (and hence the intensity $\langle a^+ a \rangle = |\alpha_0|^2$ in units of the average number of photons) of the signal mode. One is the vanishing solution, which corresponds to the subthreshold radiating mode at the spontaneous noise level, while the other solution is nonvanishing and corresponds to the above-threshold radiating mode. In the latter case the result for the semiclassical signal-mode intensity at the cavity output, $I^{\text{out}} = 2\gamma|\alpha_0|^2$ (without allowing for the negligible contribution of quantum fluctuations in their linear approximation), has the form

$$I^{\text{out}} = \frac{4\gamma^2}{\chi} [d - (J_1 + J_2) + \sqrt{J_1 J_2 - 1}]. \quad (21)$$

The corresponding stationary phase φ_0 of the signal mode ($\alpha_0 = |\alpha_0| \exp(i\varphi_0)$) is given by

$$\sin(\varphi_1 + \varphi_2 - 2\varphi_0) = (J_1 J_2)^{-1/2}, \quad (22)$$

where φ_1 and φ_2 are the phases of the pump fields $E_{1,2} = \sqrt{I_{1,2}} \exp(i\varphi_{1,2})$.

When $J_1 = J_2 \equiv J$, the stability range of the specified steady-state solution is determined by the inequalities

$$J_A < J < J_B \quad \text{if } \sqrt{3} < d < 2, \quad (23a)$$

$$1 < J < J_B \quad \text{if } d > 2, \quad (23b)$$

where

$$J_{A,B} = \frac{1}{3} (2d \mp \sqrt{d^2 - 3}). \quad (24)$$

The quantity J_A is the threshold value of the pump intensity parameter J , and J_B is the value at which the system returns to the radiating mode at the spontaneous noise level: $J < J_A$ and $J > J_B$ correspond to conditions for a stable nonvanishing steady-state solution, and over these ranges the semiclassical intensity is zero: $I^{\text{out}} = 0$.

We see that the above-threshold lasing mode sets in when the cavity's detuning Δ is greater than $\sqrt{3}\gamma$. Note that I^{out} vanishes at $J > J_B$ because of phase cross-modulation. Indeed, as the equations of motion imply, the role of phase cross-modulation reduces to replacing the ordinary cavity detuning $\Delta_{\text{eff}} = \Delta - \chi(I_1 + I_2)$ (see (6)). As the pump intensities I_1 and I_2 grow, Δ_{eff} diminishes, which carries the system away from the resonant mode of operation (in relation to the cavity's natural frequency ω_c).

We also note that the existence of a stable above-threshold lasing mode under conditions of inexhaustible sources of pump radiation results from phase self-modulation of the signal mode. Let us discuss this point in greater detail. In four-wave mixing with inexhaustible sources of pump radiation but without allowance for phase self-modulation of the signal mode, the only stable steady-state solution vanishes, which corresponds to the subthreshold radiating mode. When the threshold is passed, the vanishing solution loses stability and the system goes to an unstable nonstationary lasing mode with a signal-mode intensity that increases exponentially in time. Phase self-modulation leads to the emergence of a stable above-threshold lasing mode by the negative-feedback principle in the following manner. Because of this the signal-mode phase acquires an increment proportional to the number of photons in the mode. Hence an increase in the instantaneous number of photons for $J > J_A$ violates the phase-locking condition, which precludes efficient parametric amplification of the cavity mode during the mode's subsequent passage through the nonlinear medium. As a result of this compensation, the intensity of the signal mode stabilizes at the nonvanishing value given by Eq. (21).

Bistability, threshold behavior, and dependence on the nonlinearity parameter

The above results of the semiclassical approximation imply that for $d > 2$ the regions of stable vanishing and nonvanishing steady-state solutions overlap, resulting in optical bistability. Examples of the behavior of the normalized intensity $\chi I^{\text{out}}/4\gamma^2$ as a function of J are depicted in Fig. 1 (curve 3).

At the same time, numerical analysis of (15)–(17) suggests that the corresponding dependence in nonlinear quantum theory is not hysteretic. Such behavior is the result of the general nature of bistable systems (see, e.g. Ref. 27) and corresponds to a strictly statistical interpretation of the quantum mechanical mean intensity.

An approach that is logically equivalent to the quantum statistical description of optical bistability involves the appropriate (quasi)probability distribution function of either a general potential or the corresponding metastable states (see Refs. 1b and 27). In this approach, a detailed study of bistability requires investigating quantum tunneling effects and analyzing the characteristic times, statistically speaking, that the system takes to reach the steady state. However, this problem requires special treatment for the nonlinear system we are considering here, and its solution lies outside the scope of the present paper. Qualitatively, the problem can be interpreted on the basis of the results of Sec. 7 for the distri-

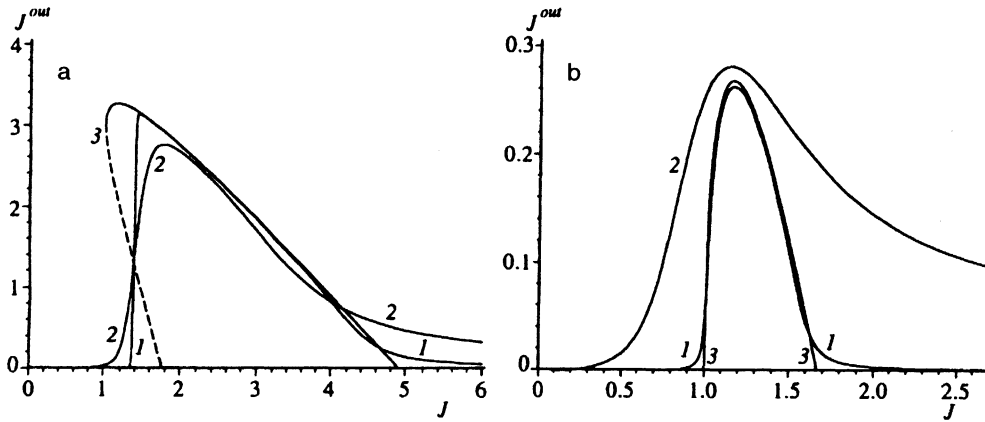


FIG. 1. Normalized signal-mode intensity at the cavity output, $J^{\text{out}} \equiv (\xi/4\gamma^2)I^{\text{out}}$, as a function of the pump intensity parameter $J = (\chi/\gamma)I$. Curves 1 and 2 represent the results of nonlinear quantum theory: (a) $d=5$ and $\delta=0.025$ (curve 1); and (b) $d=2$ and $\delta=0.01$ (curve 1) and $\delta=0.1$ (curve 2). Curve 3 represents the results of the semiclassical approximation (with the corresponding values of d); the dashed part of curve 3 in Fig. 1(a) corresponds to the unstable steady-state solution.¹⁹

bution function of the number of photons in the cavity.

Concluding this section, we note the nature of the threshold behavior of I^{out} for different values of the nonlinearity parameter $\delta = \chi/4\gamma$. Generally speaking, the common definition of a lasing threshold as a critical point in nonlinear optics systems emerges from the analysis of semiclassical solutions and their stability regions. In this sense the lasing threshold for the system under investigation is determined by the value of J_A (see (20)). Here Eq. (17) readily shows that the semiclassical result for the normalized intensity $\chi I^{\text{out}}/4\gamma^2$ expressed in terms of the dimensionless pump intensity $J = cJ = cI/\gamma$ is independent of χ/γ . Thus, the parameter δ is a scaling factor and, in addition, determines the range of J over which the linear approximation of quantum fluctuations is applicable: the smaller the value of δ , the broader the range of J , up to a small neighborhood of the system's critical points, in which the results of the linearized theory are valid; conversely, the larger the value of J , the larger the neighborhood of critical points within which these results are inapplicable.¹⁾

In nonlinear quantum theory, we see (Fig. 1) that instead of a lasing threshold there is a critical, or threshold, region. Here the signal-mode intensity I^{out} increases considerably at values of J smaller than J_A . At the same time, $\chi I^{\text{out}}/4\gamma^2$ depends explicitly on $\delta = \chi/4\gamma$. The smaller the χ/γ , the closer the transition to a lasing mode with a significant non-vanishing intensity is to a jump (numerical analysis shows that such a situation is realized up to values of $\chi/\gamma \sim 0.1$ at $d=5$, and at smaller values of χ/γ for smaller d 's).

In this case the threshold "value" of J (in the region where $\chi I^{\text{out}}/4\gamma^2$ experiences a jump) proves to be well-defined. As χ/γ increases, the $\chi I^{\text{out}}/4\gamma^2$ vs. J curve in the critical transition region becomes smoother, and relating such behavior to a threshold loses all meaning (cf. curves 1 and 2 in Fig. 1). This agrees with the results obtained below for quantum fluctuations of the number of signal-mode photons and the second-order correlation function.

5. QUANTUM FLUCTUATIONS OF THE NUMBER OF PHOTONS AND PHOTON CORRELATION

Let us now turn to the quantum statistical characteristics of the signal mode in a steady-state lasing mode. To this end we present the results of analyzing the Fano factor

$$F = \frac{\langle\langle \Delta n \rangle^2\rangle}{\langle n \rangle}, \quad (25)$$

which characterizes the variance of the number of signal-mode photons, with $\langle\langle \Delta n \rangle^2\rangle = \langle\langle (a^+ a)^2 \rangle\rangle - \langle a^+ a \rangle^2$, and the normalized second-order correlation function

$$g^{(2)} = \frac{\langle a^+ a^+ a a \rangle}{\langle a^+ a \rangle^2}. \quad (26)$$

The quantities F and $g^{(2)}$ are linked by the obvious relationship

$$F = 1 + \langle a^+ a \rangle (g^{(2)} - 1), \quad (27)$$

and their shared typical properties for chaotic, coherent, and nonclassical light fields are well-known (see, e.g., Refs. 12, 13, 28, and 29).

Using the general expressions for the moments (see Eqs. (13) and (14)) and transformations similar to those employed in calculating I^{out} , we arrive at the following expression for the correlation function $g^{(2)}$:

$$g^{(2)} = \frac{M'_{22} M'_{00}}{(M'_{11})^2}, \quad (28)$$

where the moment M'_{22} is given by

$$M'_{22} = \frac{J_1 J_2}{4} \sum_{k=0}^{\infty} \frac{(2k+1)!!}{(2k)!!} (2k+1) (J_1 J_2)^k \left(\prod_{j=1}^{k+2} P_j \right)^{-1}, \quad (29)$$

and M'_{00} , M'_{11} , and P_j are given by Eqs. (16)–(18). Having such an expression for $\langle a^+ a \rangle = M'_{11}/M'_{00}$ we can easily go from the correlation function $g^{(2)}$ to the Fano factor (27).

The results of a numerical analysis of the correlation function $g^{(2)}$ and the Fano factor F as functions of the pump intensity parameter J are depicted in Fig. 2 for various values of δ and d . A general feature of the behavior of $g^{(2)}$ is that there is a supergrouping of photons ($g^{(2)} \gg 1$) for values of J below the critical region. This property reflects the pair production of photons belonging to the lased signal mode in the parametric four-wave mixing process. Above the critical region, in which the average intensity of the signal mode increases considerably and phase self-modulation becomes important, the function $g^{(2)}$ becomes less than unity (for small δ), which indicates nonclassical antigrupping of pho-

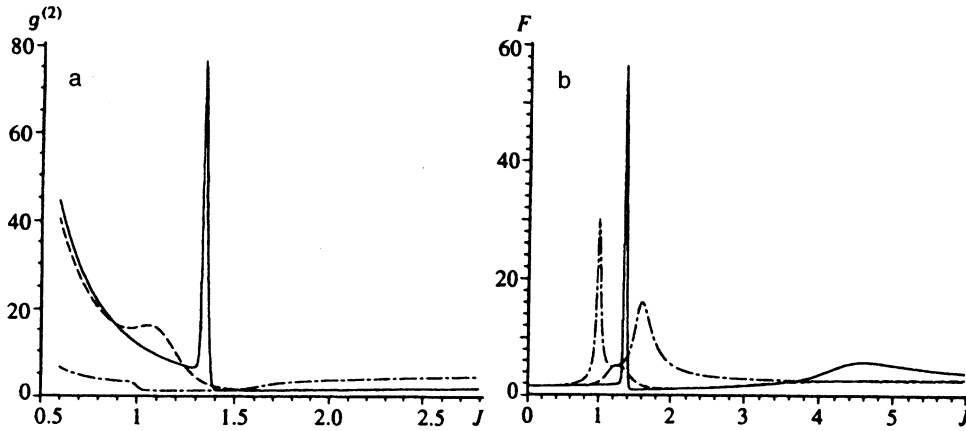


FIG. 2. The correlation function $g^{(2)}$ (a) and Fano factor F (b) as functions of J . Here $d=5$ and $\delta=0.025$ (solid curves), $d=5$ and $\delta=0.25$ (dashed curves), and $d=2$ and $\delta=0.001$ (dot-dash curves).

tons. Photon antigrouping in this region is accompanied by suppression of quantum fluctuations of the number of photons in comparison to fluctuations in the coherent state ($\langle(\Delta n)^2\rangle < \langle n \rangle$), i.e., the photons obey sub-Poisson statistics. To characterize the effect of fluctuation suppression quantitatively, we must examine the Fano factor F . For instance, for $\delta=5$ and $\delta=0.01$ the minimum of F proves to be roughly 0.82, and occurs at $J \approx 1.43$, while for $d=10$ and $\delta=0.001$ we have $F \approx 0.67$ at $J \approx 2.26$. As δ increases and d decreases, suppression of fluctuations in the number of photons worsens.

As we move away from the critical region ($J > J_B$) substantially, photon correlation acquires grouping features ($g^{(2)}$), which can be related to the fact that in this region the system reverts to radiation at the level of spontaneous noise.

Now let us return to the results in the critical threshold region. Here for small values of the nonlinearity parameter $\delta = \chi/4\gamma$, the Fano factor has a sharp peak, which suggests a sharp increase in quantum fluctuations and sub-Poisson statistics for the photons ($F \gg 1$). For instance, for $d=5$ and $\delta=0.1$, the peak value of F (at $J \approx 1.36$) is roughly 57. Note that the value of J corresponding to the peak in the Fano factor lies in the range where the $\chi I^{\text{out}}/4\gamma^2$ vs. J curve is steep (cf. the corresponding curves in Figs. 1 and 2b). This value can be identified (for small χ/γ) with the lasing threshold in nonlinear quantum theory. But as χ/γ grows, the situation changes—the peak becomes lower and broader. Hence the threshold nature of the behavior of the nonlinear system—which is determined by the characteristic features in the shape of the intensity curves and by the behavior of the fluctuations in the number of photons—loses all meaning in nonlinear quantum theory with large nonlinearities.

We also note that the increase in fluctuations or in the peak of the Fano factor at small χ/γ also exists in the vicinity of the second critical point of the system, $J = J_B$. But at the same value of χ/γ , this peak is less evident than the peak in the vicinity of the lasing threshold, which is due to a weaker variation of the intensity J^{out} in the vicinity of $J = J_B$.

One interesting feature of the behavior of $g^{(2)}$ in the critical regions must be noted. Just like the Fano factor, in the bistable lasing mode the function $g^{(2)}$ exhibits a sharp peak (for small values of χ/γ) in the near-threshold region.

However, in the vicinity of the second critical point J_B , and in the vicinity of J_A in the absence of bistability, no peak shows up in the function $g^{(2)}$. At the same time, in the Fano factor, as noted earlier, the peak behavior in critical regions is present irrespective of whether or not there is bistability. We have therefore discovered that the critical increase in $g^{(2)}$ in the near-threshold region is not related directly to the increase in fluctuations of the number of photons; instead, it is a reflection of the bistable behavior of the system.

6. SQUEEZING OF FLUCTUATIONS OF THE QUADRATURE COMPONENT

In this section we analyze the nonclassical squeezing of the fluctuations of the quadrature component of the signal mode,

$$X^\vartheta = a e^{-i\vartheta} + a^\dagger e^{i\vartheta},$$

where ϑ is the arbitrary phase of the reference wave. The effect consists in the suppression of the mean-square fluctuations

$$\langle(\Delta X^\vartheta)^2\rangle = 1 + 2\langle a^\dagger a \rangle + 2|\langle a^2 \rangle| \cos(\arg\langle a^2 \rangle - 2\vartheta) \quad (30)$$

below the level of vacuum fluctuations: $\langle(\Delta X^\vartheta)^2\rangle < 1$. Here we have allowed for the fact that the average amplitude of the signal mode, $\langle a \rangle$, is zero, which follows directly from the general expression for moments with $m=0$ and $n=1$.

If we employ Eqs. (13), (14), and (19), we arrive at an expression for the anomalous correlation $\langle a^2 \rangle$:

$$\langle a^2 \rangle = \frac{M'_{02}}{M'_{00}}, \quad (31)$$

$$M'_{02} = -\frac{1}{2} \sqrt{I_1 I_2} e^{i(\varphi_1 + \varphi_2)} \left\{ \sum_{k=0}^{\infty} \left[\frac{(2k+1)!!}{(2k)!!} \right. \right. \\ \left. \left. \times (J_1 + J_2 - d + \delta + 2k\delta)(J_1 J_2)^k \left(\prod_{j=1}^{k+2} P_j \right)^{-1} \right] \right. \\ \left. + i \sum_{k=1}^{\infty} \left[\frac{(2k+1)!!}{(2k)!!} (J_1 J_2)^k \left(\prod_{j=1}^{k+2} P_j \right)^{-1} \right] \right\}, \quad (32)$$

where φ_1 and φ_2 are the pump field phases, we have employed the notation (18) and (20), and M'_{00} is defined in (16). Hence, if we select the phase

$$\vartheta = \frac{1}{2}(\arg\langle a^2 \rangle - \pi) = \frac{1}{2}\left(\arg\frac{M'_{02}}{M'_{00}} - \pi\right) \quad (33)$$

corresponding to the minimum variance (30), we get

$$\begin{aligned} \langle (\Delta X^\vartheta)^2 \rangle_{\min} &= 1 + 2\langle a^+ a \rangle - 2|\langle a^2 \rangle| \\ &= 1 + 2\left(\frac{M'_{11}}{M'_{00}} - \frac{|M'_{02}|}{M'_{00}}\right), \end{aligned} \quad (34)$$

where M'_{11} is defined in (17).

Figure 3 shows $\langle (\Delta X^\vartheta)^2 \rangle_{\min}$ as a function of $J = \chi I / \gamma$ for various values of $d = \Delta / \gamma$ and $\delta = \chi / 4\gamma$. Analysis of (34) shows that in the absence of bistability ($d < 2$), fluctuations of the quadrature components are squeezed over the entire range of J . When bistability is present, there is a critical increase in fluctuations above the vacuum level in the threshold region, and a return of the squeezing effect in the above-threshold region. Squeezing peaks in the vicinity of the second critical point (e.g., for $d=5$ and $\delta=0.1$ we have $\langle (\Delta X^\vartheta)^2 \rangle_{\min} \approx 0.57$, i.e., the squeezing amounts to 43% at $J \approx 5$) and, as we see, significant suppression of fluctuations is observed over a broad range of pump intensities. For the sake of comparison, we note that in conventional parametric frequency division of light in a cavity (see, e.g., Ref. 16) significant squeezing can only be observed in the threshold region, and as the pump intensity increases, squeezing rapidly decreases. We also note that increasing the nonlinearity parameter $\delta = \chi / 4\gamma$ worsens the squeezing effect.

7. PHOTON NUMBER DISTRIBUTION

For a fuller analysis of the quantum statistical characteristics of the signal mode, we now calculate the distribution function of the number of photons in the cavity, $p(n) = \langle n | \rho | n \rangle$, in a steady-state lasing mode. Using the P -representation (4) of the density matrix, we find that

$$p(n) = \frac{1}{n!} \int_C \int_{C'} d\alpha d\beta P(\alpha, \beta) \alpha^n \beta^n e^{-\alpha\beta}. \quad (35)$$

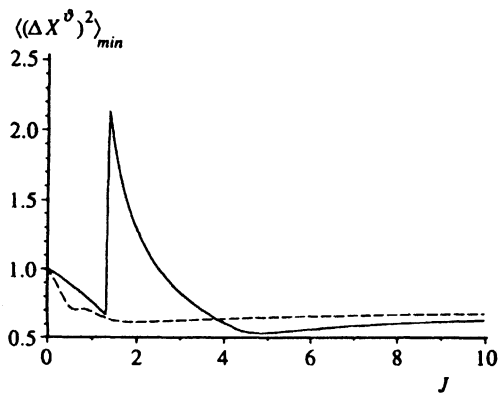


FIG. 3. The minimum variance of fluctuations of the quadrature component $\langle (\Delta X^\vartheta)^2 \rangle_{\min}$ as a function of J . Here $d=5$ and $\delta=0.025$ (solid curve), and $d=2$ and $\delta=0.25$ (dashed curve).

Plugging this into the expression (9) for the steady-state distribution $P_s(\alpha, \beta)$ and integrating by the method discussed in Sec. 3, we obtain

$$p(n) = \frac{G_{nn}}{n! M'_{00}}, \quad (36)$$

where

$$\begin{aligned} G_{nn} &= |2E_1 E_2|^n \sum_{k=0}^{\infty} \frac{|2E_1 E_2|^k}{k!} [1 + (-1)^{k+n}]^2 \\ &\quad \times \text{B}\left(\lambda + 1, \frac{k+n+1}{2}\right) \text{B}\left(\lambda^* + 1, \frac{k+n+1}{2}\right), \end{aligned} \quad (37)$$

and M'_{00} is defined in Eq. (14), where we must set $n=m=0$. For convenience of analysis, we transform Eq. (37) by using the well-known relationship between the beta function and the gamma function and the properties of the latter. The final expressions for integer n are

$$p(n) = \frac{g(n)}{n! M'_{00}}, \quad (38)$$

where

$$\begin{aligned} g(n=0) &= \frac{1}{1 + (J_1 + J_2 - d - \delta)^2} \\ &\quad + \sum_{k=1}^{\infty} \frac{[(2k-1)!!]^2}{(2k)!} \left(\frac{J_1 J_2}{4}\right)^k \left(\prod_{j=1}^{k+1} P_j\right)^{-1}, \end{aligned} \quad (38a)$$

$$\begin{aligned} g(n=2m) &= \sum_{k=0}^{\infty} \frac{[(2k+2m-1)!!]^2}{(2k)!} \left(\frac{J_1 J_2}{4}\right)^{k+m} \\ &\quad \times \left(\prod_{j=1}^{k+m+1} P_j\right)^{-1}, \end{aligned} \quad (38b)$$

$$\begin{aligned} g(n=2m-1) &= \sum_{k=1}^{\infty} \frac{[(2k+2m-3)!!]^2}{(2k-1)!} \left(\frac{J_1 J_2}{4}\right)^{k+m-1} \\ &\quad \times \left(\prod_{j=1}^{k+m} P_j\right)^{-1}, \end{aligned} \quad (38c)$$

and M'_{00} and P_j are defined in (16) and (18), respectively.

The results of numerical analysis, which are depicted in Fig. 4, show that the following features in the behavior of the distribution $p(n)$ for various values of the pump intensity parameter J and fixed values of δ and d are the most general. For values of J that are lower than those in the critical threshold region, the function $p(n)$ has a peak at $n=0$, in accordance with the spontaneous nature of emission below the lasing threshold. In the above-threshold region, $p(n)$ consists of a single "hump" with the most likely value of n differing from zero, which guarantees that the average number of photons $\langle n \rangle = \langle a^+ a \rangle = \sum_n n p(n)$ is nonzero. Here, in accordance with the sub-Poisson statistics of the photons in this region (see Sec. 5), the distribution $p(n)$ proves to be narrower than for a Poisson distribution with the corresponding value of $\langle n \rangle$. As J grows (and approaches J_B), the hump moves toward vanishing values of n and its width increases.

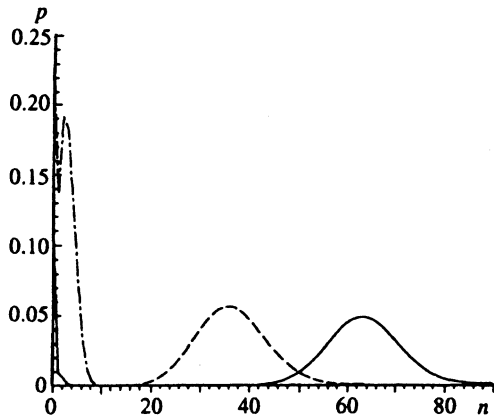


FIG. 4. Distribution function of the number of photons in the cavity, $p(n)$: $d=5$, $\delta=0.025$, and $J=1.4$ (solid curve); $d=5$, $\delta=0.025$, and $J=3$ (dashed curve); and $d=5$, $\delta=0.5$, and $J=1.66$ (dot-dash curve).

For $J > J_B$ the peak in $p(n)$ again occurs at $n=0$, which means that the system has returned to the radiating mode at the level of spontaneous noise because of phase cross-modulation.

Let us now follow the $p(n)$ curve in the threshold region, where the semiclassical intensity exhibits bistable behavior. In this region, in addition to the peak at $n=0$, there emerges a second local maximum (hump) at $n \neq 0$. The height of the second local hump grows with J (within the limits of variation of J , from $J \approx 1.36$ to $J \approx 1.42$, for the case of $d=5$ and $\delta=0.025$ depicted in Fig. 4) and at the same time the probability at $n=0$ decreases. As a result we get two local maxima at $n=0$ and $n \neq 0$ on the curve $p(n)$ (or two most likely values of n). These most likely values of n correspond to the lower and upper stable branches of the semiclassical intensity curve, while the local minimum between them corresponds to the unstable section of the semiclassical curve. The relationship between $p(n)$ and the semiclassical result for the intensity of the signal mode in the cavity can be demonstrated even more transparently by building the curve representing the dependence of the position of the local maxima and the local minimum on J (see Fig. 5). We see that for small values of δ the given curve fits the semiclassical curve fairly well. At the same time, as the nonlinearity parameter δ increases, the curve corresponding to the most and least likely values shifts in relation to the semiclassical result.

In the distribution function $p(n)$ an increase in δ shifts the position of the second hump toward smaller values of n , which lowers the absolute value of $\langle n \rangle = \sum_n n p(n)$. Moreover, an increase in δ leads to a situation in which the two local maxima coexist over a much broader range of J . This leads to a smoother nonthreshold behavior of the intensity curve I^{out} in the critical transition region, in accordance with the results of Sec. 4.

8. WIGNER FUNCTION

Studying nonclassical states of light often involves, in addition to the distribution $P(\alpha, \beta)$ and other distributions, the Wigner function $W(\alpha)$. In the case of a single-mode light field,

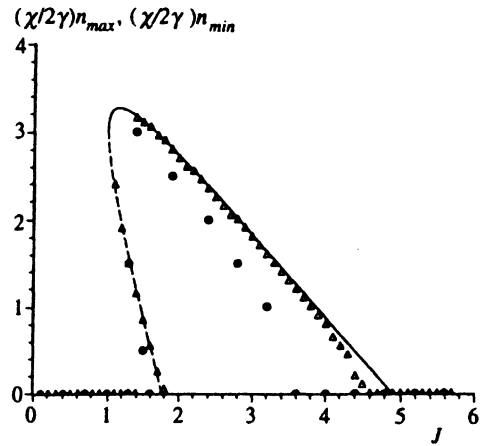


FIG. 5. The dependence of the values of n corresponding to the maxima and the local minimum between the maxima (provided that there are two local maxima in the bistable mode) of the distribution $p(n)$ on the pump intensity parameter J at $d=5$: Δ corresponds to $\delta=0.025$, and \bullet to $\delta=0.25$. The specified most likely and least likely values are plotted with a scaling factor $\chi/2\gamma$; for the sake of comparison the result for the semiclassical intensity $J^{\text{out}} = (\chi/4\gamma^2)I^{\text{out}}$ is also given (see curve 3 in Fig. 1a); it is expressed in terms of the number of photons in the cavity, $n_0 = |\alpha_0|^2$, in the semiclassical approximation on the same scale $(\chi/4\gamma^2)I^{\text{out}} = (\chi/2\gamma)n_0$. The distribution maxima lie near the stable branches of the semiclassical intensity curve, and the minima lie near the unstable branch.

$$W(\alpha) = \frac{1}{\pi^2} \int d^2\gamma \text{Tr}[\rho \exp(\gamma a^+ - \gamma^* a)] \times \exp(\gamma^* \alpha - \gamma \alpha^*). \quad (39)$$

For certain problems, the Wigner function has certain advantages over other quasiprobability distributions. In particular, being a function of a single complex variable—the joint quasiprobability distribution of the two quadrature components (“coordinate” and “momentum”) $x = \text{Re}\alpha$ and $p = \text{Im}\alpha$ —it has proved convenient in analyzing the properties of nonclassical states of light in phase space. Furthermore, and importantly, the Wigner function can be experimentally reproduced by optical homodyne tomography³⁰ by measuring the distribution of the quadrature components of the light field. Thus far, it has been reproduced for a light field in the vacuum state and for squeezed light obtained via parametric frequency division of the light in a $\chi^{(2)}$ -nonlinear crystal.^{31,32} This stresses the importance of theoretically analyzing the properties of the Wigner function for specific nonlinear optics systems with allowance for quantum fluctuations and dissipation.

For the nonlinear system under consideration, the Wigner function can be calculated using the function $P(\alpha, \beta)$. Our calculations show that the function is quite simple. Indeed, starting with the definition and passing to normal ordering of operators and the P -representation (4), we find that the function $W(\alpha)$ is linked to $P(\alpha, \beta)$ by an integral transformation,

$$W(\alpha) = \frac{2}{\pi} \exp(-2|\alpha|^2) \times \int_C \int_{C'} d\delta d\beta P(\delta, \beta) \exp(2\alpha\beta + 2\alpha^*\delta - 2\delta\beta). \quad (40)$$

Note that in obtaining this result we used the integral

$$\int d^2\gamma \exp(-s|\gamma|^2 - \mu\gamma^* + \nu\gamma) = \frac{\pi}{s} \exp\frac{\mu\nu}{s},$$

with $\text{Re } s > 0$.

Plugging the expression (9) for the steady-state distribution function into (40), we note that the exponential factor $\exp(-2\delta\beta)$ in (40) is canceled by the factor $\exp(2\delta\beta)$ in the function $P_s(\delta, \beta)$, which leads to separation of the variables in the respective contour integrals. This simplifies integration considerably and, making use of the integral representation of the Bessel function $J_\nu(z)$ (with the same integration contours as in (12); see Ref. 25), we arrive at the following result in the steady-state lasing mode:

$$W_s(\alpha) = N \exp(-2|\alpha|^2) \frac{|J_{\lambda+1/2}(2\alpha^* \sqrt{2E_1 E_2})|^2}{|(\alpha^*)^{\lambda+1/2}|^2}. \quad (41)$$

Here the inessential constant factors that appear in the integration have been absorbed into the normalization constant N .

The Wigner function can assume both positive and negative values. The fact that $W(\alpha)$ can be positive is a manifestation of the nonclassical nature of the light field. In particular, $W(\alpha)$ assumes negative values for Fock and superposition states.^{12,13} In this connection we note that the Wigner function (41) obtained for the four-wave interaction process considered here is positive over the entire range of α .

9. CONCLUSION

One of the main features of the nonlinear optics system considered in this paper is that it can achieve an above-threshold single-resonance mode of lasing of nonclassical light with low energy exchange between the pump fields and the signal mode. Such an "uncommon" lasing mode (in the absence of exhaustion of the pumping source) is realized because, in addition to parametric four-wave mixing, we allow for phase self-modulation of the signal mode, which has a profound stabilizing effect above threshold. We believe this is important in selecting this system as a highly stable generator of squeezed and sub-Poisson light.

Below are some remarks concerning the fundamental aspects of our results.

What is important is that for the given system we were able to find a steady-state quasiprobability distribution $P_s(\alpha, \beta)$ as an exact solution of the Fokker-Planck equation in the complex-valued P -representation, and could carry out an exact quantum statistical analysis without resorting to lin-

earization in quantum fluctuations. As a result we have thoroughly studied the intensity, photon correlation effects, variance of the number of photons and of phase-dependent quadrature components, and distribution of the number of photons. The results can be applied at an arbitrary level of quantum noise and in the lasing threshold region. Understandably, with this approach we attempted primarily to study large values of χ/γ , at which the level of quantum noise is high and the exact quantum results differ significantly from the corresponding approximate results of the linearized theory.

As Secs. 5 and 6 show, an increase in χ/γ leads to a worsening in both the nonclassical squeezing of fluctuations of the quadrature component and the sub-Poisson statistics of the photons. Moreover, instead of the lasing threshold as a critical point of the nonlinear system in the semiclassical theory, in exact quantum theory there emerges a critical region of behavior of physical quantities. Here, although the hysteretic dependence of the steady-state intensity I^{out} disappears as a result of exact quantum statistical averaging, bistability manifests itself in the distribution function $p(n)$ in the form of two local maxima in the critical transition region. As χ/γ increases, $\chi I^{\text{out}}/4\gamma^2$ rises more smoothly as a function of J in the critical region, and may even start at zero. Clearly, identifying such behavior with a threshold makes no sense.

The quantum "threshold" behavior can be analyzed by studying the Fano factor, which has a sharp peak in the critical regions, due to a significant increase in the level of quantum fluctuations. But for this quantity too, threshold behavior shows up only at small values of χ/γ and disappears when χ/γ becomes larger.

To better illustrate these results, we used $\chi/\gamma \sim 0.001-1$ in our numerical analysis. In real physical systems this ratio is lower; in particular, in high- Q cavities and atomic gases the ratio may reach $\sim 10^{-7}-10^{-8}$ at best (at $\chi^{(3)} \sim 10^{-8}$ esu and $\gamma \sim 10^6$ s⁻¹), although for highly nonlinear condensed media (liquid crystals), χ/γ can be higher.

Among the interesting results of the present work is the behavior of the correlation $g^{(2)}$ in the critical region, where $g^{(2)}$ has a sharp peak only if the system is bistable. To our knowledge, we have identified critical growth of the pairwise correlation of photons for parametric processes in the near-threshold lasing region for the first time. For instance, for parametric lasing in a $\chi^{(2)}$ -medium (three-frequency interaction) the behavior of $g^{(2)}$ in the threshold region was studied in Refs. 14 and 15, but only in the absence of a bistable lasing mode. As a result, $g^{(2)}$ exhibited no singularity in the threshold region, considered as a function of the pump intensity.

It is also important, we believe, that we found an exact analytic expression for the Wigner function $W(\alpha)$, the joint quasiprobability distribution of the two quadratic components of the light field, $x = \text{Re } \alpha$ and $p = \text{Im } \alpha$. Of course, this result requires further study. We also note that for parametric processes that allow for energy dissipation, the Wigner function has only been calculated approximately for three-frequency parametric lasing.³³

The authors are grateful to V. O. Papyan and K. G. Petrosyan for useful discussions.

¹¹For numerical estimates in the general case, one must turn to calculations of the quantum fluctuations of the intensity and the signal-mode phase in Ref. 19.

- ¹P. D. Drummond, K. J. McNell, and D. F. Walls, (a) *Optica Acta* **27**, 321 (1980); (b) *Optica Acta* **28**, 211 (1981).
- ²S. Reynaud, C. Fabre, and E. Giacobino, *J. Opt. Soc. Am. B* **4**, 1520 (1987).
- ³A. S. Lane, M. D. Read, and D. F. Walls, *Phys. Rev. A* **38**, 788 (1988).
- ⁴M. D. Reid and P. D. Drummond, *Phys. Rev. A* **40**, 4493 (1989).
- ⁵Yu. M. Golubev and V. N. Gorbachev, *Opt. Spektrosk.* **64**, 638 (1988) [*Opt. Spectrosc. (USSR)* **64**, 380 (1988)].
- ⁶M. J. Collett and D. F. Walls, *Phys. Rev. A* **32**, 2887 (1985).
- ⁷C. M. Savage and D. F. Walls, *J. Opt. Soc. Am. B* **4**, 1514 (1987).
- ⁸D. C. Sanders and M. D. Reid, *Phys. Rev. A* **42**, 6767 (1990).
- ⁹M. Brambilla, F. Castelli, L. A. Lugiato *et al.*, *Opt. Commun.* **83**, 367 (1991).
- ¹⁰G. Yu. Kryuchkyan and K. V. Kheruntsyan, *Quant. Opt.* **4**, 289 (1992).
- ¹¹L. A. Lugiato, G. Strini, and F. deMartini, *Opt. Lett.* **8**, 256 (1983).
- ¹²C. W. Gardiner, *Quantum Noise*, Springer, Berlin (1991).
- ¹³D. F. Walls and G. J. Milburn, *Quantum Optics*, Springer, Berlin (1994).
- ¹⁴P. D. Drummond and C. W. Gardiner, *J. Phys. A* **13**, 2353 (1980).
- ¹⁵P. D. Drummond and D. F. Walls, *J. Phys. A* **13**, 725 (1980).
- ¹⁶G. J. Milburn and D. F. Walls, *Opt. Commun.* **39**, 401 (1981).
- ¹⁷K. J. McNeil and C. W. Gardiner, *Phys. Rev. A* **28**, 1560 (1983).
- ¹⁸G. Yu. Kryuchkyan, K. G. Petrosyan, and K. V. Kheruntsyan, *Kvant. Elektron. (Moscow)* **22**, 599 (1995).
- ¹⁹G. Yu. Kryuchkyan and K. V. Kheruntsyan, *Quant. Semiclass. Opt.* **7**, 529 (1995).
- ²⁰D. Grandclement, M. Pinard, and G. Grynberg, *IEEE J. Quantum Electron.* **25**, 560 (1989).
- ²¹J. F. Reintjes, *Nonlinear Optical Parametric Processes in Liquids and Gases*, Academic Press, New York (1984).
- ²²S. A. Akhmanov and M. A. Vorontsov (eds.), *New Physical Principles of Processing Optical Data* [in Russian], Nauka, Moscow (1990).
- ²³W. H. Louisell, *Quantum Statistical Properties of Radiation*, Wiley, New York (1973).
- ²⁴C. W. Gardiner, *Handbook of Stochastic Methods. For Physics, Chemistry and the Natural Sciences*, 2nd ed., Springer, Berlin (1985).
- ²⁵D. S. Kuznetsov, *Special Functions* [in Russian], Vysshaya Shkola, Moscow (1965).
- ²⁶M. J. Collett and C. W. Gardiner, *Phys. Rev. A* **39**, 1386 (1984).
- ²⁷L. A. Lugiato, in *Progress in Optics*, Vol. 21, E. Wolf (ed.), North-Holland, Amsterdam (1984), p. 69.
- ²⁸D. N. Klyshko, *Physical Foundations of Quantum Electronics* [in Russian], Nauka, Moscow (1986).
- ²⁹D. F. Smirnov and A. S. Troshin, *Usp. Fiz. Nauk* **153**, 233 (1987) [*Sov. Phys. Usp.* **30**, 851 (1987)].
- ³⁰R. Vogel and H. Risken, *Phys. Rev. A* **40**, 2847 (1989).
- ³¹D. T. Smithey, M. Beck, M. G. Raymer, and A. Faridani, *Phys. Rev. Lett.* **70**, 1244 (1993).
- ³²G. Breitenbach, T. Muller, S. F. Pereira, J.-Ph. Poizat, S. Schiller, and J. Mlynek, *J. Opt. Soc. Am. B* **12**, 2304 (1995).
- ³³P. Kinsler and P. D. Drummond, *Phys. Rev. A* **43**, 6194 (1991).

Translated by Eugene Yankovsky